

Analysis of Circular Plate on Elastic Half-space – A Coupled FE-BE Approach

J.J. Mandal[†] and D.P. Ghosh[‡]

Introduction

The flexural behaviour of finite plates resting on elastic half-space is of interest in the analysis and design of raft foundation. The analysis of finite plates should take into consideration both continuity conditions at the interface and boundary conditions prescribed at the edges of the plate. An analytical description of the interaction problem related to the finite plates should take into account the following factors.

- (i) The type of the plate
- (ii) The type of the supporting medium
- (iii) The types of the boundary conditions
- (iv) The types of loading

As far as the analysis of circular plate on elastic half-space is concerned, the earlier method of analysis (Borowicka, 1936, 1939; Gorbunov-Possadov, 1941) is based on representation of contact stress by means of power series in terms of the radial co-ordinate, limited to a finite number of terms. Zemochkin (1939) analysed the axisymmetric problem of a circular plate resting on elastic half-space by considering compatibility of displacements between elastic halfspace and the plate along a series of concentric circular regions. Brown (1969) analysed a uniformly loaded circular plate, resting on elastic half-space. It was demonstrated that for the plate with large relative

[†] Assistant Professor, Department of Civil Engineering, Regional Engineering College, Silchar -- 788 010, India.

[‡] Professor, Department of Civil Engineering, Indian Institute of Technology, Kharagpur – 721 302, India.

stiffness, the maximum moment varies to a large extent with the number of terms included in the power series solution. Hemsley (1987) determined the flexural response of an elastic circular raft, for different types of ground support in the form of prescribed contact pressures. Results show wide disparity in the computed raft behaviours using different ground models.

The application of finite element technique to the circular raft in friction-less contact with an isotropic layer is presented by Hooper (1974). Hooper (1975) extended the solution to account for the transverse isotropy of the soil medium. Varadarajan and Arora (1982) investigated a circular footing resting on the surface of sand by stress dependent non-linear finite element method. Melerski (1997) presented a numerical technique for elastic interaction between an axisymmetric circular raft and cross-anisotropic media by finite element method.

Boundary integral equation method is used to investigate the plate on elastic foundations (Winkler model) for different edge conditions by Katsikadelis and Armenakas (1984). Puttonen and Varpusuo (1986) used the boundary element method to investigate circular plate problems on elastic foundations (one and two parameter) for different loading conditions. Katsikadelis and Kallivokas (1986) used the boundary element method for analysis of clamped circular plates on Pasternak-type elastic foundation. Sapountzakis and Katsikadelis (1992) applied the boundary element method for analysis of simply supported and clamped thin circular plates for linear as well as non-linear variation of sub-grade reaction. Wang Jianguo et al. (1993) analysed clamped thick circular plates on a Winkler foundation. All the analyses are restricted to Winkler or two parameter foundation models and for a plate having different boundary conditions. They have used direct boundary element formulation for the solution of the problems.

The Present Study

In this present paper, a FE-BE (finite element-boundary element) coupling technique is used to analyse the circular plate on elastic half-space problems. The half-space response is based on the solution given by Mindlin (1936) for a point load in half-space, which allows to take into account the effect of embedment of the plate. The plate and the half-space are two separate models in unilateral and frictionless contact at the interface. Plate-half-space interface is discretised into two dimensional isoparametric quadrilateral quadratic elements and the plate is discretised into eight noded isoparametric plate bending finite elements (Figs. 1a and 1b) based on Mindlin's plate bending theory which allows for transverse shear deformation. Each node of the plate-bending element has three degrees of freedom, namely vertical displacement and two orthogonal rotations (Fig. 2a). It can be used for both thin and thick plates; the deformation of the plate in XZ plane is

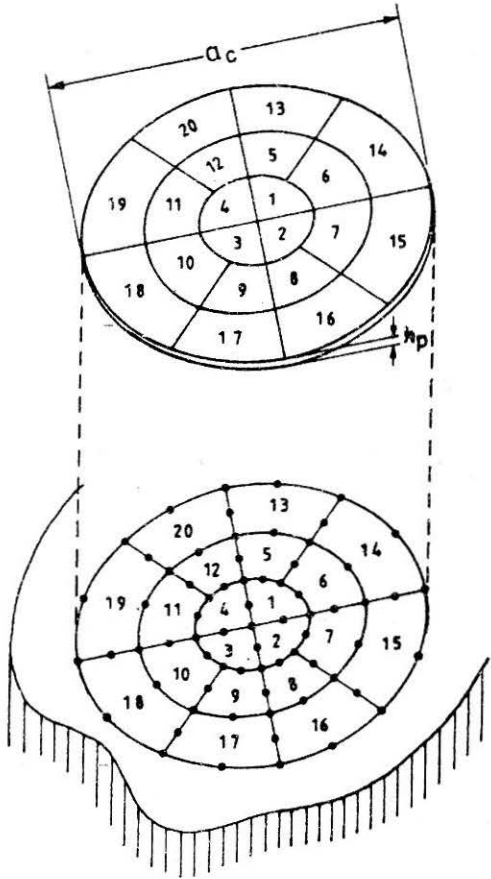


FIGURE 1(a) : Circular Plate on Elastic Continuum – Discretisation of Soil Foundation System in Plate Finite Elements and Soil Boundary Elements

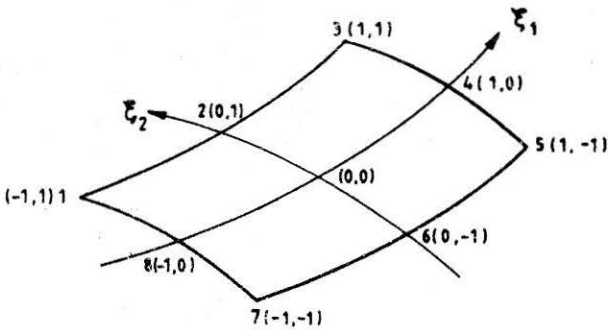


FIGURE 1(b) : Two-Dimensional Isoparametric Quadrilateral Quadratic Element

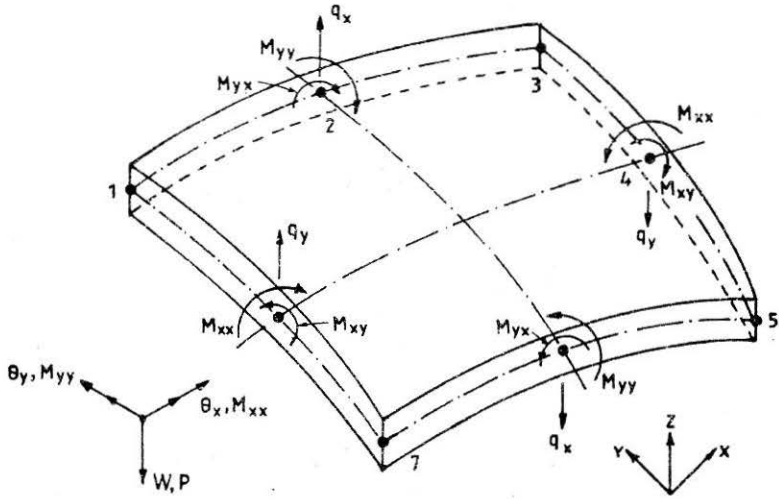


FIGURE 2(a) : Degrees of Freedom and Stress Resultants for the Isoparametric Plate Bending Finite Element

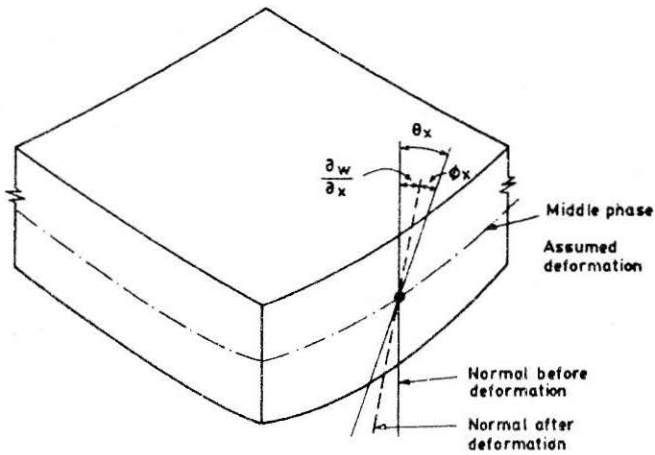


FIGURE 2(b) : Deformation of the Plate in XZ Plane

shown in Fig. 2(b). The same discretisation scheme is used for the half-space to maintain a node to node correspondence between the plate and the half-space. The stiffness matrix obtained from the boundary element method (by inverting the flexibility matrix) is coupled with the plate stiffness matrix obtained from finite element method after proper transformation to get stiffness matrix of the plate-half-space system. Thus a solution can be obtained for any load distribution on the plate. Once the deformations of the plate are obtained the stresses can be obtained by back substitution. Reduced and selective integration techniques are used to get appropriate results.

A computer programme is developed on the basis of the procedure described above in which discretisation is automatic and requires very nominal data input. It allows for most of the practical load cases and produces accurate results. With slight modification it can be used for plate of any shape and flexibility. The effectiveness and the usefulness of the proposed method and the developed computer programme are demonstrated by numerical examples.

Mathematical Formulation

Due to the singularities in the expressions from the Mindlin's solution for the displacement, it is not possible to constitute the stiffness matrix in its usual sense. On the other hand, the displacement field due to a distributed load obtained by integration of these expressions over a finite area is regular everywhere. Hence, it is possible to express the nodal displacements in terms of nodal stress intensities. This relation may be evaluated by directly integrating the Mindlin's singular expressions (1936) for a concentrated load. The Cartesian displacement vector at a point P due to traction distributed over an infinitesimal area $ds(Q)$ at Q may be written as:

$$du_i(P) = U_{ij}(P, Q) t_j(Q) ds(Q) \quad (1)$$

where $U_{ij}(P, Q)$ represents the displacement at P in the i th direction due to traction $t_j(Q)$ in the j th direction at Q. Integrating over the entire half-space-structure interface the expressions for displacement at P may be written as:

$$u_i(P) = \int_s U_{ij}(P, Q) t_j(Q) ds(Q) \quad (2)$$

The traction vector at an arbitrary point Q is related to the corresponding nodal components by the interpolation:

$$t_i(Q) = N_c(t_j)_c \quad (3)$$

where N_c = shape function and

$(t_j)_c$ = corresponding traction at the nodal point.

So the Eqn. (2) can now be written as:

$$u_i(P) = \int_s U_{ij}(P, Q) N_c(t_j)_c ds(Q) \quad (4)$$

In the present formulation the boundary (surface) of the solution domain is divided into a number of interconnected two-dimensional isoparametric quadrilateral quadratic elements. In the natural co-ordinate system the equation takes the form

$$u_i(P) = \sum_{m=1}^M \sum_{c=1}^8 (t_j)_c \int_{-1}^{+1} \int_{-1}^{+1} U_{ij}(P, Q) N_c(\xi_1, \xi_2) J(\xi_1, \xi_2) d\xi_1 d\xi_2 \quad (5)$$

where $J(\xi_1, \xi_2)$ = Jacobian of transformation and

M = total number of elements.

Integrating the above expression for each node one by one and after subsequent assembly in the global array, the displacement vector may be put in the form

$$\{(u_i)_c\} = [A] \{(t_i)_c\} \quad (6)$$

where $\{(u_i)_c\}$ = nodal displacement,

$\{(t_i)_c\}$ = stress intensity vectors,

$[A]$ = soil flexibility matrix.

As the displacement vanishes as $r \rightarrow \infty$, the rigid body mode is naturally excluded from the solution. Hence, the relation between the distributed nodal stress parameter $(t_i)_c$ and displacement $(u_i)_c$ is unique and non-singular. Thus the inverse relation can be expressed as:

$$\{(t_i)_c\} = [A]^{-1} \{(u_i)_c\} \quad (7)$$

Coupling of BE and FE Matrices

For coupling BE & FE matrices, nodal tractions should be transformed into equivalent nodal forces. This can be done by equating the work done over an element by equivalent nodal forces and tractions. It is possible to write a transformation matrix $[M]$ to transform the global nodal forces to global nodal traction vectors.

$$\{(F_i)_c\} = [M]\{(t_i)_c\} \quad (8)$$

where $\{(F_i)_c\}$ = nodal force vectors due to half-space reaction.

Now Pre-multiplying Eqn. (7) by $[M]$

$$[M]\{(t_i)_c\} = [M][A^{-1}]\{(u_i)_c\} \quad (9)$$

or

$$\{(F_i)_c\} = [MA^{-1}]\{(u_i)_c\}$$

But, neither the nodal force vectors nor the displacements are known till the nodal force vectors are related to the externally applied loads. These relationships are derived from equations of equilibrium as described below.

Isoparametric plate bending elements are used in the present formulation. They can be used for analysis of both thin and thick plates. The same discretisation is used as for the boundary element so that a node to node correspondence is obtained. As explained earlier, the half-space contact pressure is represented by nodal force vectors at the nodes. So from the kinematics of the plate-half space system, it can be written as:

$$K_p \{(u_i)_c\} = -\{(F_i)_c\} + \{P_o\} \quad (10)$$

where K_p = assembled stiffness matrix of the plate,

$\{(u_i)_c\}$ = generalised displacement at the nodes and

$\{P_o\}$ = applied external load at the nodes.

Substituting the value of $\{F_i\}_c$ from Eqn. (9)

$$\begin{aligned}
 K_p \{(u_i)_c\} &= -[MA^{-1}]\{(u_i)_c\} + \{P_o\} \\
 \Rightarrow [K_p + MA^{-1}]\{(u_i)_c\} &= \{P_o\} \\
 \Rightarrow \{(u_i)_c\} &= [K_p + MA^{-1}]^{-1}\{P_o\} \\
 \Rightarrow \{(u_i)_c\} &= [K_{ps}]^{-1}\{P_o\}
 \end{aligned} \tag{11}$$

where $[K_{ps}] = [K_p + MA^{-1}] =$ combined stiffness matrix

By solving the above equation displacement parameters can be obtained.

Computation of Stresses

Once the displacement parameters are known, the stresses can be found out by back substitution. In the finite element analysis using the displacement method, the stresses are discontinuous between the elements, because of the nature of the assumed displacement variation. Experience has shown that in case of isoparametric elements the integration (Gauss) points are the best stress sampling points. The nodes, which are the most useful points for the outputs and interpretation of stresses, appear to be the worst sampling points. Barlow (1976) has shown that for two dimensional isoparametric elements the 2 by 2 Gauss integration points are optimal stress sampling points. Local stress smoothing technique as demonstrated by Hinton & Campbell (1974) is used to extrapolate stress values computed at Gauss points to nodal points. $\sigma_1 \dots \sigma_8$ are smoothed nodal values and $\sigma_1 \dots \sigma_{1V}$ are the stresses at Gauss points as shown in the Fig. 3(b).

In the computer programme, the smoothed stress resultants are then modified by finding the average of the nodal stress resultants of all the elements meeting at a common node.

Numerical Examples and Discussions of Results

On the basis of the mathematical formulation and numerical procedures presented in the previous sections, a computer program has been developed to analyse the elastostatic contact between a circular plate and homogeneous elastic half-space.

For presentation and discussion of results it is appropriate to use a

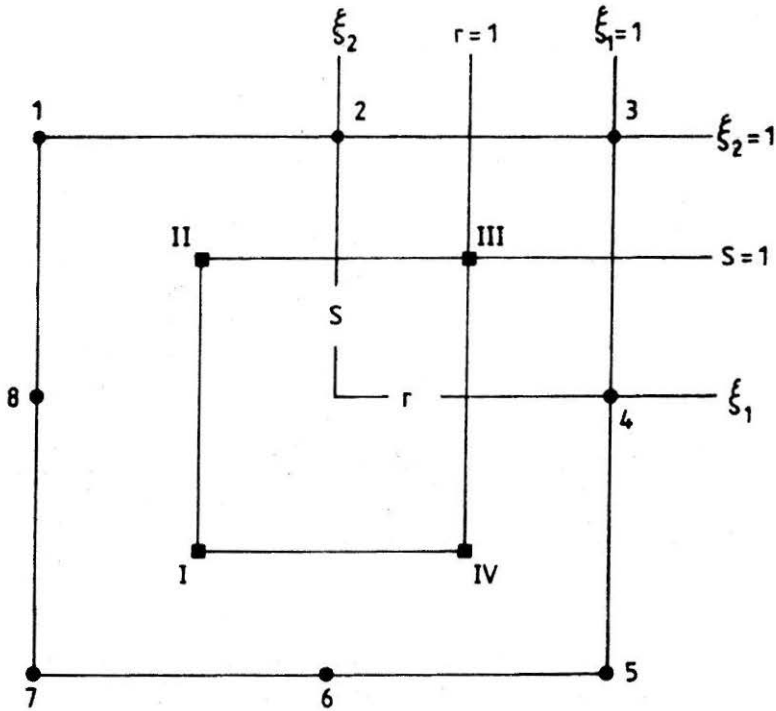


FIGURE 3(a) : Natural Co-ordinate System used in Extrapolation of Stresses from Gauss Points

$$\begin{bmatrix} \sigma_1 \\ \sigma_2 \\ \sigma_3 \\ \sigma_4 \\ \sigma_5 \\ \sigma_6 \\ \sigma_7 \\ \sigma_8 \end{bmatrix} = \begin{bmatrix} -0.500 & 1.866 & 0.134 & -0.500 \\ -0.183 & 0.683 & -0.183 & 0.683 \\ 0.134 & -0.500 & -0.500 & 1.866 \\ -0.183 & -0.183 & 0.683 & 0.683 \\ -0.500 & -0.134 & 1.866 & -0.500 \\ -0.683 & -0.183 & 0.683 & -0.183 \\ 1.866 & -0.500 & -0.500 & -0.134 \\ 0.683 & 0.683 & -0.183 & -0.183 \end{bmatrix} \begin{bmatrix} \sigma_{\text{I}} \\ \sigma_{\text{II}} \\ \sigma_{\text{III}} \\ \sigma_{\text{IV}} \end{bmatrix}$$

$\sigma_{\text{I}} \dots \sigma_{\text{IV}}$ - Gauss point values

$\sigma_1 \dots \sigma_8$ - Nodal point values

FIGURE 3(b) : Extrapolation Matrix to Obtain Nodal Stresses from Gauss Point Stresses (Hinton and Campbell, 1974)

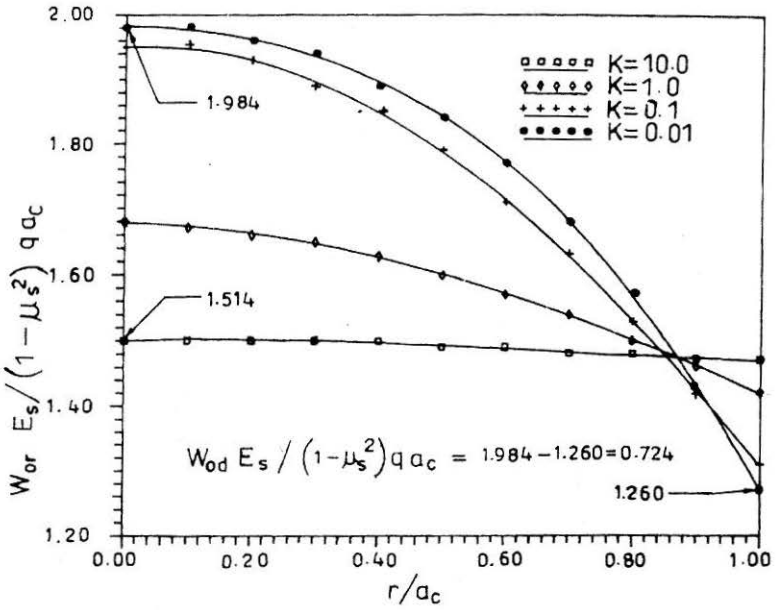


FIGURE 4 : Vertical Displacement of a Uniformly Distributed Circular Plate Resting on Elastic Half-space ($\mu_s = \mu_p = 0.15$)

relative stiffness parameter, K , for the plate-elastic half-space system [as used by Brown (1969)]

$$K = \left[\frac{E_p (1 - \mu_s^2)}{E_s} \right] (h_p / a_c)^3$$

where E_s = elastic modulus of the half-space,
 μ_s = Poisson's ratio,
 h_p = thickness,
 E_p = modulus of elasticity and
 a_c = radius of the plate.

When the value of the parameter $K = 0$, the plate can be considered to be a completely flexible one, and $K = 100$ represents a very stiff plate (almost rigid).

The vertical deflections for different relative stiffness parameter under a uniformly distributed load are shown in Fig. 4.

Completely flexible plate on homogeneous half-space

The bounding solutions for a completely flexible plate are given by those cases where the load is applied directly to the half-space (elastic constants E_s and μ_s). For a uniform stress q applied normal to the surface over a circular area of radius a_c , from the Boussinesq equations maximum surface displacement W_{or} and maximum differential surface displacement between the centre and edge of the loaded area W_{od} can be written in the non-dimensional form by

$$W_{or} E_s / [1 - \mu_s^2] q a_c = 2.0, \quad \text{and}$$

$$W_{od} E_s / [1 - \mu_s^2] q a_c = 0.727$$

respectively. The corresponding values by the present formulation are 1.984 and 0.714 respectively (Fig. 4).

Completely rigid plate on homogeneous half-space

For frictionless contact, from the Boussinesq equation for normal surface displacement W_{or} for the loaded surface is

$$W_{or} E_s / (1 - \mu_s^2) q a_c = \pi/2(1.57)$$

The corresponding value by the present formulation is 1.514 (Fig. 4)

Plate with finite flexibility on homogeneous half-space

The differential deflections with relative plate stiffness are compared with the corresponding values obtained by Brown (1969) for plate Poisson's ratio (μ_p) = 0.15 in Fig. 5(a). In Fig. 5(b) the variation of the differential deflections with relative plate stiffness is shown, for values of μ_p = 0.15 and 0.3. The differential deflection changes rapidly with plate stiffness in the region near $K = 1$.

The radial moment (M_r) distributions with relative plate stiffness are compared with the corresponding values obtained by Brown (1969) for plate Poisson's ratio (μ_p) = 0.30 in Fig. 6(a). In Fig. 6(b) the variations of bending moments (M_r and M_t) with relative plate stiffness' are shown for values of plate Poisson's ratio = 0.3.

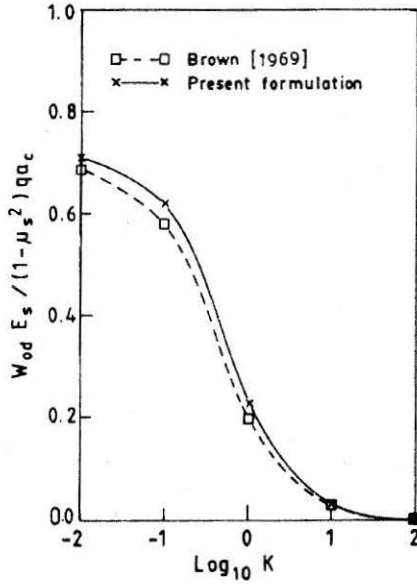


FIGURE 5(a) : Comparison Differential Deflection with Plate Stiffness of a Uniformly Loaded Circular Plate Resting on Elastic Half-space ($\mu_s = \mu_p = 0.15$)

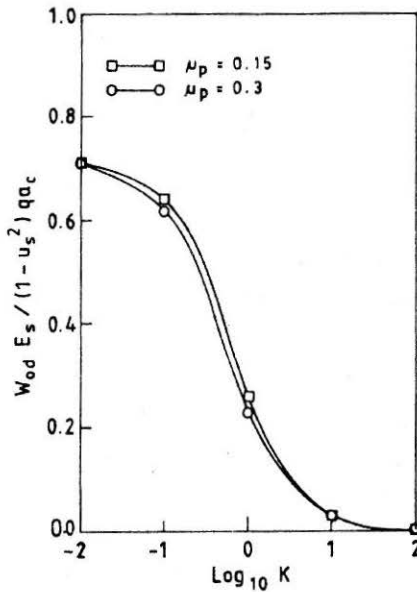


FIGURE 5(b) : Variation of Differential Deflection with Plate Stiffness of a Uniformly Loaded Circular Plate Resting on Elastic Half-space ($\mu_p = 0.30$ and $\mu_p = 0.15$)

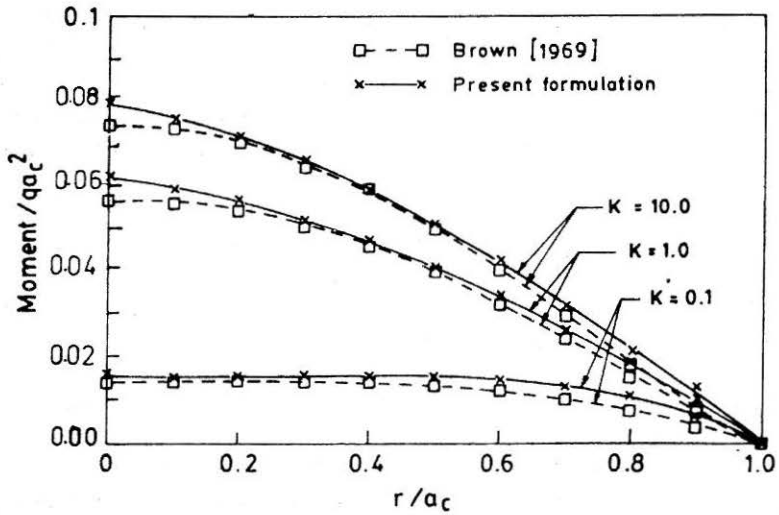


FIGURE 6(a) : Comparison of Radial Moment Distribution (M_r) for Various Plate Stiffnesses of a Uniformly Loaded Circular Plate Resting on Elastic Half-space ($\mu_p = 0.30$)

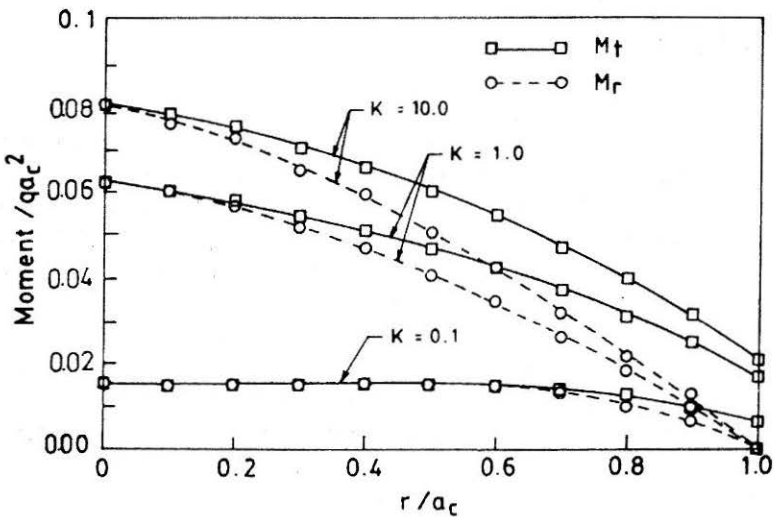


FIGURE 6(b) : Bending Moment Distribution (M_r and M_t) for Various Plate Stiffnesses of a Uniformly Loaded Circular Plate Resting on Elastic Half-space ($\mu_p = 0.30$)

Maximum moments are compared for different stiffness parameters with the values obtained by Brown (1969) in Fig. 7(a). The variation of the maximum moments with relative plate stiffness is shown for values of plate Poisson's ratio = 0.15 and 0.3 in Fig. 7(b). As with the differential deflection, the maximum moment changes rapidly with plate stiffness in the region near $K = 1$.

The comparison of the computed results with those obtained by Brown (1969) shows the applicability of the present formulation for wide range of rigidity of the plate in terms of relative stiffness parameters and plate Poisson's ratio.

Effect of plate thickness and depth of embedment on response

To study the influence of plate thickness on response, an analysis is carried out for a centrally loaded (5000 kN) circular raft of diameter 6m, Poisson's ratio = 0.2 and elastic modulus = 0.25×10^5 MN/m², resting on a soil having modulus = 25 MN/m² and Poisson's ratio = 0.3, for different plate thickness's. The results are graphically presented in Fig. 8.

The effect of embedment depth on the settlement for a particular raft-soil system (same as above with a thickness of 0.7 m) is shown in Fig. 9. The settlement reduces with increase in the depth of embedment. So a choice of depth of embedment for a particular raft-soil system can be made for a permissible value of settlement depending upon the serviceability.

Conclusion

The FE-BE coupled approach can be used very effectively in the solution of unilateral contact between plates and elastic half-space foundations. The results presented here amply demonstrated the accuracy of the proposed numerical method. It utilises the advantages of finite element and the boundary element techniques by coupling. It is devoid of problems encountered in finite element analysis due to the infinite extent of the half-space or representing it with Winkler foundations.

It can be used to analyse plates of any shape and size under the action of any type of load by proper discretisation. Since Mindlin's half-space solution is used as the fundamental solution, the effect of embedment of the plate in the half-space can also be considered. This is suitable for analysing both thin and thick plates resting on an elastic half-space. This formulation will be very useful for design and analysis of raft foundations since it does not impose any restriction regarding loading and thickness of the plate.

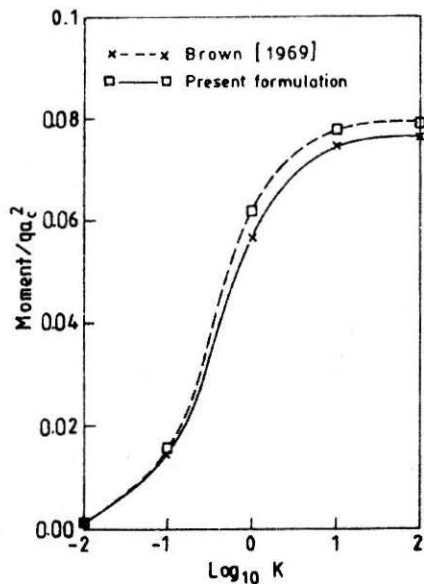


FIGURE 7(a) : Comparison of Maximum Moment with Various Plate Stiffnesses of a Uniformly Loaded Circular Plate Resting on Elastic Half-space ($\mu_p = 0.30$)

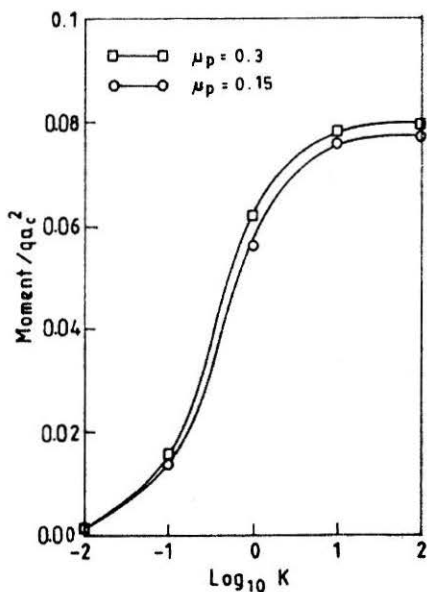


FIGURE 7(b) : Variation of Maximum Moment with Various Plate Stiffnesses of a Uniformly Loaded Circular Plate Resting on Elastic Half-space ($\mu_p = 0.30$ and $\mu_p = 0.15$)

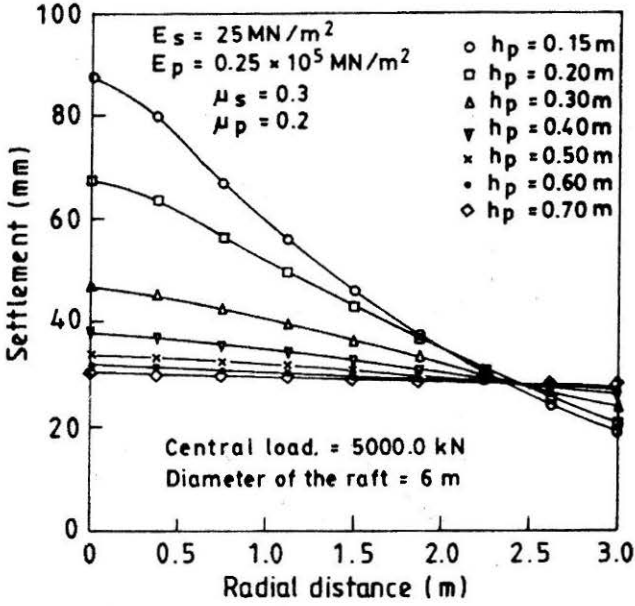


FIGURE 8 : Settlement of a Centrally Loaded Circular Raft (Effect of Thickness)

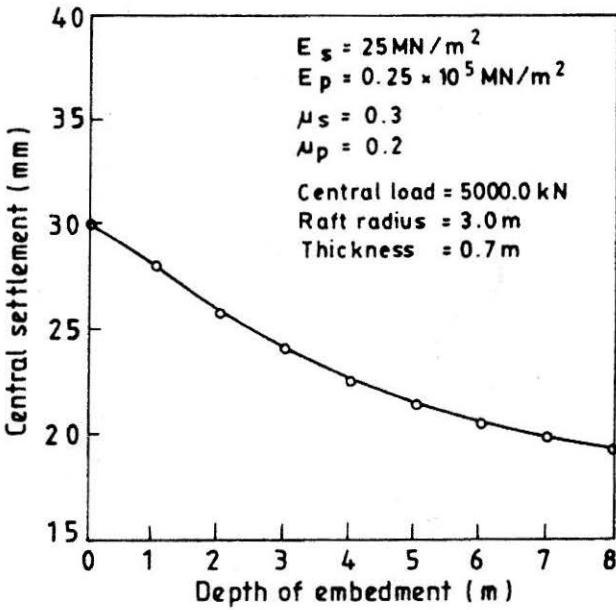


FIGURE 9 : Central Settlement of a Centrally Loaded Raft (Effect of Depth of Embedment)

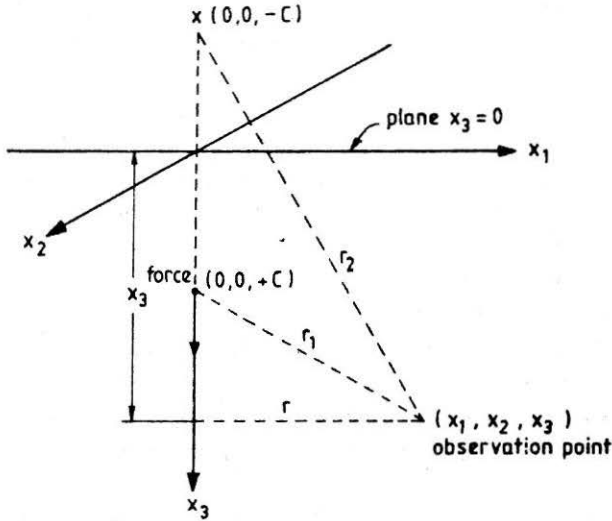


FIGURE 10 : Force Normal to Boundary in the Interior of a Semi-infinite Solid

References

- BARLOW, J. (1976) : "Optimal Stress Locations in Finite Element Method", *Int. J. Numer. Meth. Engrg.*, Vol.10, pp.243-251.
- BOROWICKA, H. (1936) : "Influence of Rigidity of a Circular Foundation Slab on the Distribution of Pressure over the Contact Surface", *Proc. 1st. Int. Conf. Soil Mech. Found. Engg.*, Vol.2, pp.144-149.
- BOROWICKA, H. (1939) : "Druckverteilung unter Elastischen Platten", *Ing. Arch.*, Vol.10, No.2, pp.113-125.
- BROWN, P.T. (1969) : "Numerical Analysis of Uniformly Loaded Circular Rafts on Deep Elastic Foundation", *Geotechnique*, Vol.19, No.3, pp.399-404.
- GORBUNOV-POSSADOV, M.I. (1941) : "Slabs on Elastic Foundations", *Gostroiizdat*, Moscow (in Russian).
- HEMSLEY, J.A. (1987) : "Elastic Solutions for Axisymmetrically Loaded Circular Raft with Free or Clamped Edges Founded on Winkler Springs or a Half-space", *Proc. Inst. Civil. Engrs.*, Part 2, 83, Mar., pp. 61-90.
- HINTON, E. and CAMPBELL, J.S. (1974) : "Local and Global Smoothing of Discontinuous Finite Element Function using a Least Square Method", *Int. J. Numer. Meth. Engrg.*, Vol.8, pp.461-480.
- HOOPER, J.A (1974) : "Analysis of a Circular Raft in Adhesive Contact with a Thick Elastic Layer", *Geotechnique*, Vol.24, No.4, pp.561-580.
- HOOPER, J.A. (1975) : "Elastic Settlement of a Circular Raft in Adhesive Contact with a Transversely Isotropic Medium", *Geotechnique*, Vol.25, No.4, pp.691-711

KATSIKADELIS, J.T. and ARMENAKAS, A.E. (1984) : "Plate on Elastic Foundation by BIE Method", *J. Engg. Mech. Div., ASCE.*, Vol.110(7), pp. 1086-1105.

KATSIKADELIS, J.T. and KALLIVOKAS, L.F. (1986) : "Clamped Plates on Pasternak-type Elastic Foundation by the Boundary Element Method", *J. Appl. Mech.*, Vol.53, pp.909-917.

MELERSKI, E.S. (1997) : "Numerical Modelling of Elastic Interaction between Circular Rafts and Cross-anisotropic Media", *Computers & Structures*, Vol.64, No.1-4, pp.567-578.

MINDLIN, R.D. (1936) : "Force at a Point in the Interior of a Semi-infinite Solid", *Physics*, Vol.7, pp.227-235

PUTTONEN, J. and VARPASUO, P. (1986) : "Boundary Element Method for Plates on Elastic Foundation", *Int. J. Numer. Meth. Engrg.*, Vol.23, pp.287-303.

SAPOUNTAZAKIS, E.J. and KATSIKADELIS, J.T. (1992) : "Unilaterally Supported Plates on Elastic Foundations by the Boundary Element Method", *J. Appl. Mech.*, ASME., Vol.58, pp.580-586.

VARADARAJAN, A. and ARORA, K.R. (1982) : "Interaction of Circular Footing - Sand Bed System", *Proceedings of the Fourth International Conference on Numerical Method in Geomechanics*, Edmonton, Canada, Vol.2, pp.945-953.

WANG JIANGUO, XIUXI, W. and MAOKUANG, H. (1993) "Boundary Integral Equation Formulation for Thick Plates on a Winkler Foundation", *Computers & Structures.*, Vol.49, No.1, pp.179-185.

ZEMOCHKIN, B.N. (1939) : "Analysis of Circular Plates on Elastic Foundation", *Mosk. Izd Voенno. Inzh. Akad* (in Russian).

Notations

- a_c = Radius of the plate/raft
 $[A]$ = Half-space flexibility matrix
 E_p = Modulus of elasticity of the plate/raft
 E_s = Modulus of elasticity of half-space
 μ_p = Poisson's ratio of the plate/raft
 μ_s = Poisson's ratio of half-space
 h_p = Thickness of the plate/raft
 $[M]$ = Transformation matrix (to transform the BE matrices to equivalent FE matrices for coupling)
 W_{or} = Radial deflection of the plate
 W_{od} = Differential deflection of the plate
 K = Relative stiffness parameter
 $\{(u_i)_c\}$ = Nodal displacement vector
 $\{(t_i)_c\}$ = Nodal traction vector
 $\{(F_i)_c\}$ = Nodal force vector due to half-space reaction
 K_p = Plate stiffness matrix
 $[A^{-1}]$ = Half-space stiffness matrix (from BEM)
 $[MA^{-1}]$ = FEM equivalent half-space stiffness matrix
 K_{ps} = Combined (plate – half-space) stiffness matrix

Appendix

Mindlin's Expressions

The X_1 and X_2 components of displacements due to the force normal to the interface U_1^* and U_2^* are given by (Fig. 10):

$$U_1^* = U_2^* = \frac{Pr}{16\pi G(1-\mu)} \left[\frac{x_3 - c}{r_1^3} + \frac{(3-4\mu)(x_3 - 3)}{r_2^3} - \frac{4(1-\mu)(1-2\mu)}{r_2(r_2 + x_3 + c)} + \frac{6cx_3(x_3 + c)}{r_2^5} \right]$$

The X_3 component of displacement U_3^* is given by:

$$U_3^* = \frac{P}{16\pi G(1-\mu)} \left[\frac{3-4\mu}{r_1} + \frac{8(1-\mu)^2 - (3-4\mu)}{r_2} + \frac{(x_3 - c)}{r_1^3} + \frac{(3-4\mu)(x_3 + c)^2 - 2cx_3}{r_2^3} + \frac{6cx_3(x_3 + c)^2}{r_2^5} \right]$$